Correlated Vibrational Dynamics Revealed by Two-Dimensional Infrared Spectroscopy

N. Demirdöven, M. Khalil, and A. Tokmakoff

Department of Chemistry, Massachusetts Institute of Technology, Cambridge, Massachusetts 02139

(Received 14 June 2002; published 15 November 2002)

Two-dimensional infrared (2D IR) spectroscopy has been used to monitor the solvent-induced correlated fluctuations in the transition energies of two coupled vibrations. The elongation of diagonal and cross peaks in a 2D IR correlation spectrum reflects the degree of inhomogeneity in the individual transition energies and the correlation between them. Changes in the 2D line shapes as a function of a variable waiting period have been successfully reproduced by a correlated spectral diffusion model.

DOI: 10.1103/PhysRevLett.89.237401 PACS numbers: 78.30.Jw, 42.50.Md, 63.50.+x, 78.47.+p

Two-dimensional (2D) infrared (IR) spectroscopies have proven to be effective at probing interactions between multiple coordinates in condensed phase systems [1–3]. Because vibrational transitions are directly related to nuclear coordinates, the positions and line shapes of the resonances in a 2D IR spectrum reveal information about molecular structure and dynamics. The formation of cross peaks reflects the coupling between different molecular coordinates and the orientations of their transition dipoles [1–3]. Solvation dynamics, encoded in the fluctuations of transition energies, and the spectral broadening due to solvent-induced disorder are characterized by 2D line shapes and their evolution as a function of an experimentally controlled waiting period [3,4]. The combination of these attributes implies a powerful tool for studying variation of conformation, solvent environment, or other disorder induced by many-body interactions in complex systems.

The sensitivity of a 2D IR spectrum to couplings between coordinates and inhomogeneous broadening indicates that the shape of cross peaks will also be sensitive to correlations in the distribution of the transition energies of coupled modes [5,6]. For two coupled coordinates, the vibrational states m and n are described by a joint inhomogeneous distribution, whose form will strongly depend on how these interactions occur at a microscopic level. The correlated shifts of the transition energies relative to the ground state $\delta\omega_{m,0}$ and $\delta\omega_{n,0}$ can be quantified by a normalized covariance factor $\rho_{mn} = \langle\delta\omega_{m,0}\delta\omega_{n,0}\rangle/\sigma_m\sigma_n$, where $\sigma_{m(n)}$ is the corresponding distribution width. ρ_{mn} varies between $+1$ and -1 indicating the degree of correlation, where a value of 0 represents no correlation [5–7]. When the interactions with the solvent shift the transition frequencies of coupled modes in opposite directions from their central values, for example, through a distribution of vibrational couplings (off-diagonal disorder), anticorrelated spectral broadening ($\rho < 0$) will occur. If the two frequencies shift in the same direction, which will be the case when the solute-solvent interactions result in a distribution of vibrational frequencies (diagonal disorder), correlated broadening will be observed ($\rho > 0$).

In this Letter, we report on a 2D IR study of time-dependent correlation effects in the solvation dynamics of coupled vibrational modes, using the time evolution of 2D line shapes to characterize correlated fluctuations. 2D IR spectroscopy is a heterodyne-detected four wave mixing technique that monitors the propagation of vibrational coherences during two time periods, an initial evolution period τ_1 and a final signal detection period τ_3, which are separated by a fixed waiting time τ_2. Three femtosecond, mid-IR, laser fields $\boldsymbol{E}_a$, $\boldsymbol{E}_b$, and $\boldsymbol{E}_c$ with incident wave vectors $\boldsymbol{k}_a$, $\boldsymbol{k}_b$, and $\boldsymbol{k}_c$ interact with the sample to generate the nonlinear signal field $\boldsymbol{E}_s$ along the phase-matched direction $\boldsymbol{k}_s = -\boldsymbol{k}_a + \boldsymbol{k}_b + \boldsymbol{k}_c$. The Fourier transform (FT) of $\boldsymbol{E}_s$ with respect to τ_1 and τ_3 gives a 2D spectrum in ω_1 and ω_3, in which peaks represent the coherent states sampled during the two time periods. By varying the time ordering of pulses along the $\boldsymbol{k}_a$ and $\boldsymbol{k}_b$ wave vectors, we detected two different signals along $\boldsymbol{k}_s$ with pulse orderings $\boldsymbol{a}$-$\boldsymbol{b}$-$\boldsymbol{c}$ and $\boldsymbol{b}$-$\boldsymbol{a}$-$\boldsymbol{c}$. These are referred to as rephasing and nonrephasing, respectively, based on the phase relationship with which vibrational coherences evolve during τ_1 and τ_3 [8]. In a rephasing (or echo) experiment, the phase acquired by coherences during the evolution period, $e^{i\Omega\tau_1}$, is the conjugate of that for the detection period, $e^{-i\Omega\tau_3}$. Coherences in nonrephasing measurements evolve with the same phase during both τ_1 ($e^{-i\Omega\tau_1}$) and τ_3 ($e^{-i\Omega\tau_3}$). The sum of these signals gives a 2D correlation spectrum with absorptive 2D line shapes [9].

The rephasing and nonrephasing spectra contain complementary information on line broadening mechanisms and correlation effects. For an inhomogeneously broadened transition, the degree of inhomogeneity is reflected in the time profile of the rephasing experiment by an echo signal formed along $\tau_1 = \tau_3$, or equivalently in the frequency domain, by the elongation of the peak along the diagonal axis ($\omega_1 = \omega_3$). In the 2D spectrum, the diagonal slice characterizes the inhomogeneous distribution, and the antidiagonal slice gives the homogeneous linewidth [10]. For a homogeneous system, the line shape is symmetric. Generally, a separation of time scales is not possible because the transition frequency fluctuates in

time. The time scale of this process can be characterized by varying the waiting period τ_2. If the correlation time, τ_c, is longer than the time scale of the experiment ($\tau_1 + \tau_2 + \tau_3$), the system appears inhomogeneous and a diagonally elongated 2D line shape is observed. As τ_2 is varied from $\tau_2 < \tau_c$ to $\tau_2 > \tau_c$, the 2D line shape will vary from diagonally elongated to symmetric.

Cross peaks in a 2D IR spectrum form by propagation under two different distributions during τ_1 and τ_3, and will therefore be sensitive to the cross correlation of frequency fluctuations within these distributions. In the case of totally correlated broadening ($\rho = +1$), the transition energy shift of one oscillator corresponds to an equal shift in the transition energy for the other. For each member of the ensemble, the phase acquired by one oscillator during τ_1 is transferred to the other oscillator, so that the memory of the frequency in the evolution period is retained in the detection period. In a rephasing experiment, the original polarization involving the first transition can be refocused, forming an echo on the second transition. This leads to a cross peak elongated parallel to the diagonal. For totally anticorrelated broadening ($\rho = -1$), the shift in energy of one oscillator is opposite to the shift in energy of the other. Then, since the phase acquired by members of the ensemble during τ_1 is transferred to the second distribution in an inverted manner, the macroscopic refocusing of the ensemble is seen in the conjugate, nonrephasing experiment. This leads to elongation of the cross peak along the antidiagonal axis. These distinct signatures of correlated and anticorrelated broadening in rephasing and nonrephasing spectra ensure that the 2D vibrational correlation spectrum, which is given by their sum, will be sensitive to both. Beyond the static picture, the correlated frequency shifts may also be time dependent, and the decay of the correlated fluctuations can be observed as the change in cross peak line shape from elongated to symmetric as the waiting time τ_2 is increased to match the cross-correlation time for the two coupled modes.

As a model system to probe the correlated solvation dynamics, we study the coupled asymmetric (a) and symmetric (s) carbonyl (C≡O) stretching modes of acetylacetonato dicarbonyl rhodium(I), or RDC, in chloroform solution. The two fundamental transitions are at $\omega_a = 2014\ \mathrm{cm}^{-1}$ and $\omega_s = 2085\ \mathrm{cm}^{-1}$ with absorption linewidths of 9.3 and 14.6 cm^{-1}, respectively (Fig. 3 inset). The room temperature sample was 5×10^{-3} M corresponding to a peak optical density of 0.25. 90 fs mid-IR pulses ($\lambda = 4.9\ \mu\mathrm{m}$; $\nu = 2050\ \mathrm{cm}^{-1}$) were split into four equivalent beams (~ 50 nJ), three of which focused into the sample in a standard box configuration. The fourth beam was further split into two to obtain a signal tracer and a local oscillator (LO) [4]. The nonlinear signal emitted from the sample was temporally and spatially overlapped with the LO field. A 190 mm grating monochromator was used to disperse the fields onto a 64-element HgCdTe array detector, for an experimental resolution of ~3 cm^{-1}. A set of temporal interferograms was obtained as a function of τ_1 in steps of ~2 fs up to 4 ps for each Fourier component of the detected signal ω_3 for both rephasing and nonrephasing experiments. The two data sets are individually cosine transformed, phased, and added to give the 2D IR correlation spectrum for a given waiting period τ_2 [9]. The data presented here were taken in the all-parallel polarization geometry.

We collected 2D IR correlation spectra of RDC in chloroform for waiting periods of $\tau_2 = 0$, 1.4 2.9, 6.2, and 9.5 ps. The waiting times were chosen to correspond to the maxima of the quantum beats at $\omega_s - \omega_a = 71\ \mathrm{cm}^{-1}$ (469 fs) that modulate the amplitude of the peaks as a function of τ_2. Figures 1(a)–1(c) show the 2D correlation spectra for $\tau_2 = 0$, 2.9, and 6.2 ps. Each spectrum exhibits two diagonal and two cross peaks, each of which are split into a pair of oppositely signed peaks. Diagonal peaks arise from processes involving one fundamental during τ_1, and the same fundamental (positive) or its overtone (negative) during τ_3. Cross peaks originate from the processes involving one fundamental during τ_1, and the other fundamental (positive) or its combination band (negative) during τ_3. For the $\tau_2 = 0$ spectrum [Fig. 1(a)], the 2D diagonal line shapes are elongated, indicating inhomogeneous broadening. The cross peaks are also elongated and tilted parallel to the diagonal, which is a sign of correlated broadening ($\rho > 0$). For increased waiting times, the elongation of both diagonal and cross peak line shapes becomes less pronounced and the tilt disappears [Figs. 1(a)–1(c) and Fig. 2]. For the cross peaks, this can be emphasized by noting the apparent rotation of the node between positive and negative features from being aligned along the diagonal to being aligned along ω_1 (Fig. 2). This change arises from a change in the relative amplitudes of peaks in the rephasing and nonrephasing spectra from a value of $A_R/A_{NR} \simeq 6$ at $\tau_2 = 0$ to a value of ~1.2 at $\tau_2 = 6.2$ ps. The angle of the tilt relative to the ω_1 axis (as drawn in Fig. 2) can be defined as $\tan(\Psi) = (A_R - A_{NR})/(A_R + A_{NR})$ [9]. These effects arise from solvent-induced frequency fluctuations that lead to a gradual loss of memory of the initial frequencies and their correlation, and are consistent with a system undergoing strongly correlated fluctuations on a picosecond time scale. An additional set of resonances observed more clearly for $\tau_2 = 6.2$ ps [Figs. 1(c) and 2(c)] most likely corresponds to a stable association of RDC and chloroform.

To model the correlated solvation dynamics of the coupled vibrations, we use exponentially decaying energy gap auto- and cross-correlation functions:

$$\zeta_{mn}(t) = \langle \delta\omega_{m,0}(t)\delta\omega_{n,0}(0)\rangle_B = \rho_{mn}\sigma_{mm}\sigma_{nn}\exp(-|t|/\tau_{mn}),$$

where $m, n = a, s$. τ_{mn} is the correlation time and ρ_{mn} is

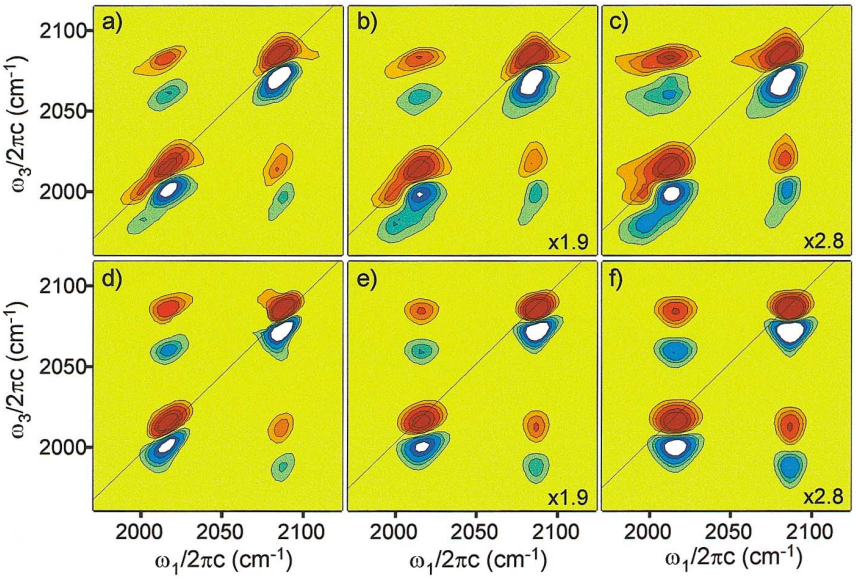

FIG. 1 (color). Experimental [(a), (b), and (c)] and best-fit [(d), (e), and (f)] 2D IR correlation spectra of RDC in chloroform for three different waiting times, $\tau_2 = 0$, 2.9, and 6.2 ps, respectively. Contour levels are 6% for the first three in each direction and 12% otherwise.

the unitless covariance factor, where $\rho_{mm} \equiv 1$. We used the harmonic approximation to express the energy gap correlation functions involving doubly excited states in terms of those involving singly excited states [11], which resulted in eight independent parameters: the correlation coefficient ρ_{as}, the amplitudes σ_a, σ_s; the correlation times τ_{aa}, τ_{ss}, and τ_{as}; and the transition dipole strengths $\mu_{a,0}$ and $\mu_{s,0}$.

The correlation function for the system-bath interaction can be used with existing treatments of the third-order nonlinear response for multilevel systems [12], and has been explicitly treated by Sung and Silbey [13]. We evaluate the nonlinear dephasing functions corresponding to Liouville pathways for a given wave vector matching condition. The total nonlinear response for rephasing and nonrephasing experiments is calculated separately as a function of τ_1 and τ_3 by summing over all corresponding pathways in the RDC six-level system, incorporating the effect of molecular reorientation on the dynamics for each period τ_1, τ_2, and τ_3 [1,14]. The responses are double Fourier transformed along τ_1 and τ_3 to give the 2D rephasing and nonrephasing spectra in ω_1 and ω_3, and added after the nonrephasing spectrum is reflected across the $\omega_3 = 0$ axis, giving the 2D correlation spectrum [9]. The global nonlinear least-squares fitting of the 2D correlation spectra for all values of τ_2 gave the following best-fit parameters: $\mu_{a,0}/\mu_{s,0} = 1.06 \pm 0.04$, $\sigma_a = 7.4 \pm 0.6\ \text{cm}^{-1}$, $\sigma_s = 5.2 \pm 0.4\ \text{cm}^{-1}$, $\tau_{aa} = 2.0 \pm 0.2$ ps, $\tau_{ss} = 2.0 \pm 0.4$ ps, $\tau_{as} = 1.2 \pm 0.4$ ps, and $\rho_{as} = 0.9 \pm 0.1$, indicating a high degree of correlation. Figures 1(d)–1(f) show the 2D correlation spectra calculated with these parameters, which successfully reproduces the experimental spectra as a function of τ_2 in terms of the tilt of the cross and diagonal peaks, their degree of elongation, absorption linewidths, and the intensities.

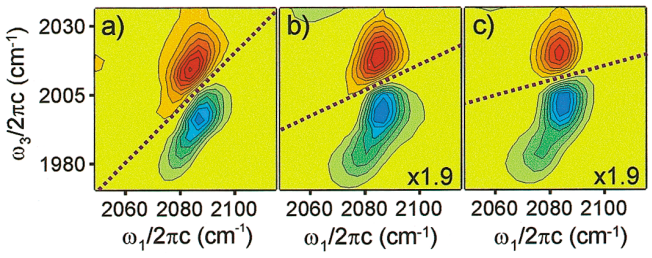

FIG. 2 (color). Sections corresponding to cross peaks at $(\omega_1, \omega_3) = (2085, 2015)$ and $(2085, 2002)\ \text{cm}^{-1}$ at $\tau_2 = 0$, 2.9, and 6.2 ps, respectively. The rotation of the node between the two resonances is emphasized by the change in the slope of the line drawn in between corresponding to $\Psi = \pi/4$, $\pi/7$, and $\pi/12$ [9]. Contour levels are in 6% intervals.

We also performed dispersed three-pulse echo peak shift (3PEPS) experiments at $\omega_3 = 2015\ \text{cm}^{-1}$ shown in Fig. 3. 3PEPS experiments have been widely used to model system-bath correlation functions for two-level systems [15]. Our experimental 3PEPS decays with two apparent time scales: a dominant, short 1.6 ps and a low-amplitude, 8 ps component. This result compares favorably with the 1.9 ± 0.2 ps decay calculated from fit parameters, which is between the two experimentally observed values because our model correlation function is a single exponential. Additionally, the calculated linear absorption spectrum using the same best-fit parameters is in excellent agreement with the FT IR absorption spectrum of RDC (Fig. 3 inset).

The magnitudes of the frequency correlation time and amplitude parameters provide a detailed picture of the dynamics associated with the system of two coupled local vibrational coordinates interacting with a solvent bath. From the elongation of the diagonal peaks in Fig. 1(a), it is clear that the system is inhomogeneously broadened. This result is consistent with the fit autocorrelation

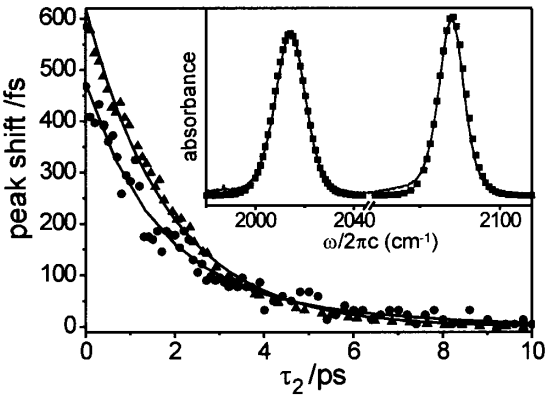

FIG. 3. Experimental (solid circles) and calculated (triangles) 3PEPS results fit to exponentials (solid lines) with decay constants 1.6 ± 0.1 and 8 ± 3 ps for experimental and 1.9 ± 0.2 ps for calculated results. The calculated (squares) and the experimental linear FT IR spectrum of RDC in chloroform are shown in the inset.

functions, which give a $\sigma \times \tau_c$ product of 2.5, indicating the slow modulation limit. Relative to the homogeneous 2D line shapes observed for RDC in hexane [1,9], RDC exhibits a considerable asymmetric broadening of the linear absorption linewidths from 2.6 cm^{-1} in hexane to > 8 cm^{-1} in chloroform (and methanol). There are two different types of solute-solvent interaction mechanisms that can induce this broadening [5]. The first mechanism is weak hydrogen bonding of chloroform to the ligand carbonyls, which is evident from the extensive broadening of the *a* and *s* C≡O stretching frequencies and the large redshifts in the C═O stretching frequencies of the acetylacetonato ligand from 1581 cm^{-1} in hexane to 1566 cm^{-1} in chloroform. The second mechanism is the dispersive electrostatic interactions between the Rh atom and the polarizable chloroform molecules. RDC is a planar (d^8) coordination compound and the nonbonding *d* orbitals of rhodium are exposed to chloroform molecules in the primary solvation shell along the two axial coordinates. Thus, the modulation of the solvent density will modulate the electron density of the Rh atom and cause the vibrational potentials of the oscillators to fluctuate due to the changes in strength of the d_π-π^* bonding. In either case, the induced distributions of *a* and *s* stretching frequencies will be correlated because the local C≡O coordinates are affected symmetrically. Although it is unclear, we think that the additional resonances arise from a solvated RDC species, which is strongly associated with chloroform along the axial position. These types of strong solute-solvent interactions could also lead to conformational changes, which would appear as a variation of coupling, or off-diagonal disorder. Clearly, the anticorrelated broadening that would mark such an effect is not present, and not expected because the vibrational coupling strength (35 cm^{-1}) [1] is significantly stronger than the solute-solvent interactions ($\sigma \sim 6$ cm^{-1}). The strong coupling of the carbonyls through the Rh atom suggests that highly correlated fluctuations can be observed in the vibrational transitions. Additional modeling in the local mode Hamiltonian [1] has shown that the asymmetric linear absorption line shapes can be explained in terms of disorder in the individual local mode anharmonicities, which reflects variation of the local solvent environment.

These results illustrate the ability of 2D spectroscopies to describe the correlated dynamics of a system of multiple coordinates with diagonal or off-diagonal disorder. The ability to investigate these effects will allow interactions within a complex system and between the system and bath to be studied selectively. Such measurements should prove to be important in the study of intramolecular and intermolecular interactions and conformational dynamics in solution, the influence of disorder on electronic excitation dynamics in light harvesting complexes and other aggregates, optical properties and carrier dynamics in semiconductors, and on many-body correlations in solids.

We thank Dr. Jaeyoung Sung for the helpful discussions on the nonlinear dephasing functions used in our theoretical modeling. This work was supported by the National Science Foundation (Grant No. CHE-0079268) and the donors to the American Chemical Society-Petroleum Research Fund.

[1] O. Golonzka *et al.*, J. Chem. Phys. **115**, 10 814 (2001).
[2] M. Zanni *et al.*, J. Phys. Chem. B **105**, 6520 (2001).
[3] S. Woutersen *et al.*, Proc. Natl. Acad. Sci. U.S.A. **98**, 11 254 (2001).
[4] J. D. Hybl *et al.*, J. Chem. Phys. **115**, 6606 (2001).
[5] N. Demirdöven *et al.*, J. Phys. Chem. A **105**, 8025 (2001); D. E. Thompson *et al.*, J. Chem. Phys. **115**, 317 (2001).
[6] N.-H. Ge *et al.*, J. Phys. Chem. A **106**, 962 (2002).
[7] S. T. Cundiff, Phys. Rev. A **49**, 3114 (1994); J. Friedrich and D. Haarer, J. Chem. Phys. **79**, 1612 (1983).
[8] C. Scheurer and S. Mukamel, J. Chem. Phys. **115**, 4989 (2001).
[9] M. Khalil, N. Demirdöven, and A. Tokmakoff (to be published).
[10] A. Tokmakoff, J. Phys. Chem. A **104**, 4247 (2000); J. D. Hybl *et al.*, Chem. Phys. **266**, 295 (2001).
[11] K. Tominaga and K. Yoshihara, Phys. Rev. A **55**, 831 (1996).
[12] S. Mukamel, Phys. Rev. A **28**, 3480 (1983).
[13] J. Sung and R. J. Silbey, J. Chem. Phys. **115**, 9266 (2001).
[14] O. Golonzka and A. Tokmakoff, J. Chem. Phys. **115**, 297 (2001).
[15] M. Cho *et al.*, J. Phys. Chem. **100**, 11 944 (1996).